Size-dependent optical properties of polyethylene powders in far-IR region: On the way to universal matrix

Liudmila A. Zhukas [a,b], Sergey L. Veber [a,b,*], Tatiana B. Mikenas [c], Maxim A. Yurkin [b,d], Elena V. Karpova [e], Valeri P. Maltsev [b,d], Viktor I. Mamatyuk [e], Ljudmila G. Echevskaya [c], Elena G. Bagryanskaya [a,b,e], Vladimir A. Zakharov [b,c]

[a] International Tomography Center SB RAS, Institutskaya str. 3a, 630090 Novosibirsk, Russia
[b] Novosibirsk State University, Pirogova 2, 630090 Novosibirsk, Russia
[c] Boreskov Institute of Catalysis, Ac. Lavrentieva ave. 5, 630090 Novosibirsk, Russia
[d] Institute of Chemical Kinetics and Combustion SB RAS, Institutskaya str. 3, 630090 Novosibirsk, Russia
[e] N.N. Vorozhtsov Novosibirsk Institute of Organic Chemistry SB RAS, Ac. Lavrentieva ave. 9, 630090 Novosibirsk, Russia

ARTICLE INFO

ABSTRACT

Similar to potassium bromide (KBr), which is used in mid-IR as a matrix for pellet preparation, polyethylene (PE) is widely applied in far-IR because it is an inert material without intensive absorption lines in this range. However, despite the material itself being transparent, the transmission of pellet made of PE powder strongly depends on the wavelength tending to decrease almost to zero in a short-wave part of the far-IR range. Heating of the pellet to PE melting temperature significantly improves its transparency, but this approach can only be applied to thermally stable compounds. In this work 8 types of PE powders of different mean particle size (MPS) ranging from 43 to 3 μm have been synthesized. Far-IR spectra of PE pellets made of these powders at room temperature have been measured and the inverse correlation between overall far-IR pellet transparency and MPS of its PE powder has been found. The imaginary part of the effective refractive index of the studied pellets obeys light-scattering scale invariance rule, indicating that the transmission of PE pellets is limited by light scattering by PE grains. It has been shown that PE powders with MPS of ∼4 μm or less are suitable as a matrix for pellet preparation in far-IR spectroscopy without the necessity of pellet melting.

© 2014 Elsevier Ltd. All rights reserved.

1. Introduction

Although the majority of infrared studies is performed in the mid-IR range (4000–400 cm^{-1}) where so-called fingerprint region for organic compounds is located, in the case of inorganic compounds a number of informative vibrational bands are shifted to the far-IR region (roughly defined as below 400 cm^{-1}). Far-IR spectroscopy has proven itself to be a valuable technique, e.g. to study the spin crossover compounds [1], phonons and plasmons in semiconductor superlattices [2], intermolecular interactions between cations and anions in ionic liquids [3] and even for analyzing inorganic pigments and corrosion products found on art objects [4,5].

If the studied compound is a solid, perhaps the most common preparation technique consists in mixing it with a matrix and pressing into a pellet. Polyethylene (PE) powder is remarkably convenient as a matrix for preparing
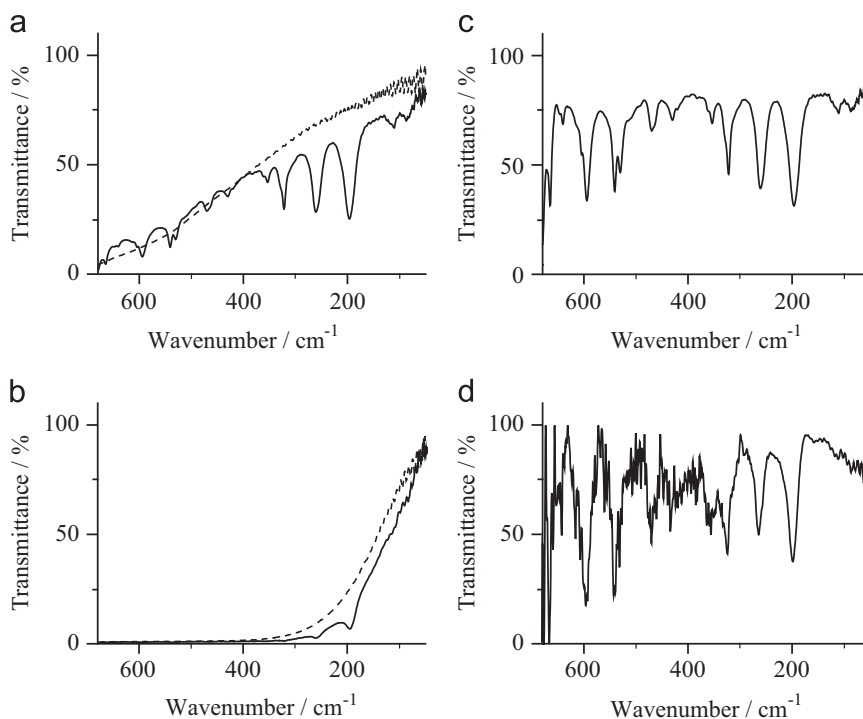
Fig. 1. Far-IR spectra of Cu(hfac)$_2$L^{Pr} compound measured using PE powders of different particle size for pellets formation: (a,b) far-IR spectra of pure PE pellets (dashed line) and pellets with a sample (solid line); (c,d) corresponding baseline corrected far-IR spectra of Cu(hfac)$_2$L^{Pr} compound.

the PE pellets for the far-IR range because PE is an inert material and it has no intensive absorption bands in the range 650 cm^{-1} to at least 33 cm^{-1} [6]. However, although the bulk PE is transparent in the far-IR range, the pellets made of PE powder disperse the far-IR radiation due to residual inhomogeneity of the compressed material. The dispersion of light strongly depends on the wavelength, tending to increase when wavelength becomes shorter. At higher wavenumbers of far-IR range the dispersion on the PE pellet can reduce the level of transmitted light almost to zero, limiting the range of spectrum that can be recorded with appropriate signal-to-noise ratio. This effect is clearly shown in Fig. 1, where the far-IR spectra of a "breathing crystal" Cu(hfac)$_2$L^{Pr} compound [7] are presented measured at room temperature using different PE powders for pellet formation (PE powders No 2 and 6 from Table 1). Samples were prepared as described elsewhere [8]. If the PE pellet itself is transparent enough in the far-IR range (Fig. 1(a), dashed line), the baseline-corrected spectra of the studied compound have high signal-to-noise ratio up to the mid-IR range (Fig. 1(c)). If not, only some part of the spectra will have satisfactory quality (Fig. 1(b) and (d)).

Insufficient transparency of the pellets made of PE powder is a well-known problem in the field of far-IR spectroscopy, and several methods have been suggested to solve it, at least to some extent. Heating of the pellet die during pellet formation up to the melting point of the PE ($\sim$130–180 C) allows one to homogenize the pellet [4,6], approaching the transmission properties of the PE matrix to bulk PE material. But this approach can be applied only for thermally stable samples. In principle,

Table 1
Transmittance limit of PE pellets in the far-IR range and mean particle size of the corresponding PE powders determined from electron microscope images (MPS-EM); peak position of the imaginary part of the effective refractive index of PE pellets and mean particle size determined by scale-invariance method (MPS-SI).

Sample number	Transmittance limit 33% (cm^{-1})	MPS-EM (μm)	Peak position for $\tilde{\kappa}(w)$ (cm^{-1})	MPS-SI (μm)
1	118	43 ± 4	255 ± 5	43[a]
2	160	34 ± 5	345 ± 5	32
3	219	14 ± 2	450 ± 10	24
4	297	3.5 ± 0.3	650 ± 50	17
5	350	4.2 ± 0.6	750 ± 50	15
6	420	3.1 ± 0.3	850 ± 10	13
7	457	3.3 ± 0.3	1080 ± 30	10
8	560	2.4 ± 0.3	1450 ± 50	8

[a] This value, by definition, equals to that in the third column.

the required temperature can be reduced down to 50 °C either by adding a wax in the PE powder [9] or by using highly linear polyethylene, which allows one to produce translucent PE pellets at room temperature without the application of heat [10]. However, these last two techniques have not been widely employed.

Commercially available PE powders that are declared suitable for far-IR spectroscopy are not well documented in this regard – at most the material description consists in mean particle size without correlation of the latter to the resulting PE pellet transparency. To the best of our knowledge, such correlation is missing in the literature, although it represents practical interest for sample preparation

technique in far-IR spectroscopy. This information becomes crucial if the studied compounds are thermally unstable and applying heat to the PE pellet is not possible.

To investigate the dependence of PE pellet transparency on the properties of PE powder, we synthesized a series of ultra-high-molecular-weight polyethylene (UHMWPE) powders of significantly different mean particle size (hereinafter referred to as MPS). Transmission spectra of the corresponding PE pellets were measured in the far-IR range and correlated with their MPS estimated on the basis of electron microscope image (hereinafter referred to as MPS-EM). Monotonic decrease of the transmittance level with the wavelength shortening was found to be the common feature for all measured PE samples, while their overall transparency in the far-IR range was substantially different. The analysis of the measured transmittance curves on the basis of scale invariance approach showed that the observed decrease of the transmittance level at higher wavenumbers is indeed caused by light dispersion on the PE powder particles, and the dispersion degree strongly depends on the particles size. Criterion for the PE powders to be suitable as pellet formation material for far-IR spectroscopy was suggested.

2. Materials and methods

2.1. Synthesis of PE powders of different MPS

PE powders of different MPS have been synthesized by the ethylene slurry polymerization in heptane over highly active supported catalysts with controlled particle size [11,12]. It is known that particle size of the polymer produced depends on the particle size of the catalyst and the yield of polymer (details are given in Appendix A) [13,14,15,16]. Employing these dependences, we have prepared eight samples of PE powders of different MPS using catalysts of MPS from ~4.5 to ~0.3 μm and variation of polymer yield from 12 to 0.7 kg per g of catalyst.

2.1.1. Imaging of PE powders and procedure of MPS-EM determination

The electron microscope TM-1000 (Hitachi High-Technologies, Japan) operating in low-vacuum regime was used to obtain images of synthesized PE powders. Each sample (PE powder) was attached to conductive adhesive tape and images with 600 and 3000 times magnification were recorded. The MPS-EM was determined as follows: on the electron microscope images of 600 or 3000 times magnification (depending on PE particle size) 20 neighboring PE grains were fitted by ellipses; their sizes were calculated as the average of main axes of corresponding ellipses; resulting MPS-EM of the PE sample is the average size value of these 20 grains and the error of MPS-EM was determined as standard deviation of measured values. In most cases the grains were agglomerated into a larger PE particle, but the sizes of individual grains were taken into account. Alternatively, we tried to measure the MPS of the studied PE powders by a MasterSizer 2000 (Malvern Instruments, UK), based on the light diffraction method, after placing the PE powder in suspension in heptane.

However, due to the strong agglomeration of powders the obtained values characterized mainly the sizes of much larger agglomerates rather than the individual grains (data not shown).

2.2. PE pellet preparation and IR spectra measurement

Transmission spectra in the far-IR range were measured at room temperature by FT-IR spectrometer Vertex 80V (Bruker Optics, Germany) equipped with a PE/DLaTGS D201 detector. Spectra were measured in the range of 50–680 cm^{-1} with a spectral resolution of 0.5 cm^{-1}. PE pellets were formed in an evacuable pellet die of 13 mm in diameter at room temperature and under the load of 7 t applied for 1 min. When the PE powder was placed into the die, the latter was pumped out by membrane pump to the pressure of 7–10 mbar during the whole compression procedure. The amount of PE powder for each pellet was 50 mg ($\pm$0.9 mg) and the resulting pellet thickness was approximately 0.5 mm.

In order to compare the transparencies of PE pellets and bulk material, we recorded the far-IR spectrum of homogeneous PE window of 1 mm thickness and recalculated the result to that of 0.5 mm thickness using the Lambert–Beer law.

For the theoretical treatment of the pellet transmission data (see below) the spectra of PE pellets in the mid-IR range (370–2000 cm^{-1}) were measured using the same spectrometer equipped with a KBr/DLaTGS D301 detector with a spectral resolution of 2 cm^{-1}.

2.3. MPS determination by light-scattering scale invariance approach

Optical density (OD, based on natural logarithm) of inhomogeneous samples (PE pellets in our case) is determined by both scattering and absorption of light waves by individual particles and their packing morphology, as well as by the optical geometry of the measuring instrument. Omitting the dependence on the latter (does not vary with samples), we can write OD=OD(w,d,h,X), where w is the wavenumber, d – MPS, h – pellet thickness. The wavenumber determines the complex refractive index $m=n+i\kappa$ of PE, where i is imaginary unit, and n, κ are real and imaginary parts of m. By X we denote all other factors of pellet morphology, including molecular structure of PE, volume fraction of PE in the pellet, shape of individual PE particles, packing structure and details of particle size distribution (not accounted for by MPS). However, we assume that X does not change significantly among the studied pellets. This assumption is reasonable considering synthesis conditions, pellet weight and dimensions (Section 2.2), and microscopic images (Fig. 3). However, it is still only an assumption, and the best justification we have is experimental verification of our theoretical prediction (e.g., Fig. 4). Moreover, we discuss the limitations of this assumption in Section 3.3.

Next, we recall the light-scattering scale invariance rule [17], which states that the result of interaction of electromagnetic wave with particle system remains the same if both the wavelength and the sizes of all particles in the

system are scaled by the same factor, keeping all refractive indices constant. The latter is important limitation, since m of PE does depend on w. However, its real part (n) is almost independent of w for $w \in [50,800]$ cm^{-1} [18,19,20]. Absorption (imaginary part of m) does depend on w, but we assume that the absorption can be completely neglected far from absorption bands. In the latter case OD is mainly determined by light scattering, i.e. we can consider m real and independent of w. Moreover, all considered particular samples do not transmit light directly, but only through multiple scattering. Except for the lowest OD, this diffuse transmittance is determined by a few first layers of the particles. Therefore, OD does not depend on h when $L \gg h \gg d$, where L is the mean absorption path that is large outside of absorption bands. Finally, for any number γ (scaling factor) we obtain

$$\mathrm{OD}(w,d,h,X) \approx \mathrm{OD}(w/\gamma, \gamma d, \gamma h, X) \approx \mathrm{OD}(w/\gamma, \gamma d, h, X), \quad (1)$$

where the first equation is the scale-invariance rule and the second equation is due to independence of OD from h. Therefore, Eq. (1) is expected to be valid under the above assumptions and describe the general shape of dependence of OD on w. Apart from absorption bands, the latter dependence is an increasing function from transparent (low OD, Rayleigh scattering) long-wavelength limit ($wd \ll 1$) to diffuse isotropic short-wavelength limit (constant OD, $wd \gg 1$).

To make this dependence more pronounced, we define the following quantity:

$$\tilde{\kappa}(w) = \frac{\mathrm{OD}(w)}{4\pi w h}, \quad (2)$$

which is, in fact, an imaginary part of the effective refractive index of the pellet, i.e. the value which will explain the observed OD if the pellet is assumed homogeneous. We stress that $\tilde{\kappa}$ is purely effective quantity; in particular, $\tilde{\kappa}$ depends on h (all other parameters being fixed). However, $\tilde{\kappa}(w)$ has a well-defined maximum for $wd = A$, where A does not depend on d due to scale invariance, given by Eq. (1). Thus, d can be easily determined from peak position in dependence of $\tilde{\kappa}$ on w, once A is known. We calibrate this approach (determine the value of A) using the sample with the largest d, for which microscopic determination of d is the least ambiguous. Unfortunately, theoretical determination of A does not seem feasible. Using this calibration a d parameter for all other samples can be calculated (hereinafter referred to as MPS-SI). MPS-SI can be considered as mean particle diameter, which is "sensed" by probing radiation, and it is important to compare this valuable parameter with the MPS determined from the electron microscope images (MPS-EM).

3. Results and discussion

3.1. Experimental data treatment and obtained correlations

The transmission spectra of pellets made of synthesized PE powders are presented in Fig. 2. In addition, the spectrum of bulk PE material of 0.5 mm thickness (the same
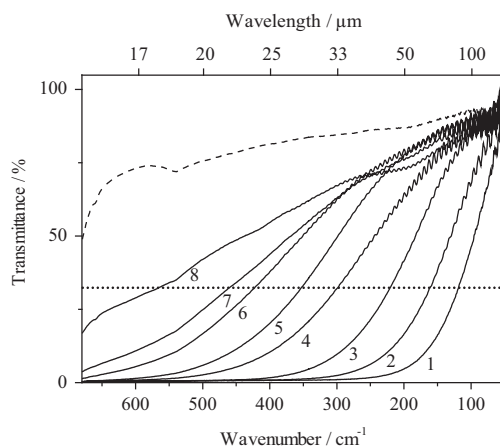
Fig. 2. Far-IR spectra of PE powders of different particle sizes pressed into pellets. Dotted line shows 33% transmittance level. Dashed spectrum represents transmittance of bulk PE material of 0.5 mm thickness.

thickness as measured PE pellets) is shown, hinting at the upper limit for the transparency of PE pellets.

Spectrum of each PE sample has two main characteristics: (i) monotonic decrease in pellet transparency with increasing wavenumber caused by increasing light scattering and (ii) transparency modulation in the low wavenumber area caused by light interference on the pellet boundaries.

In order to understand the modulation in low wavenumber area ($wd \ll 1$) the pellet can be considered homogeneous with a certain complex refractive index (computed, e.g., by an effective-medium theory [21]). However, direct fitting of interference spectra does not seem feasible due to existing surface roughness, which is even more pronounced for the bulk PE sample (Fig. 2), where such interference can be hardly observed. Nevertheless, the period of oscillations corresponds well to the pellet thickness.

The overall transparency of the measured PE samples in the far-IR range is substantially different: while sample 1 is already non-transparent at wavenumbers higher than 200 cm^{-1}, sample 8 has more than 50% transparency in the whole far-IR range and this value decreases to the 30% level only at ~600 cm^{-1}. In order to compare the transparency of the measured PE powders, we define for each sample the wavenumber that corresponds to 33% of the transmission (dotted line in Fig. 2). The numbers obtained are listed in Table 1 and lie in the wide range from 118 to 560 cm^{-1}.

Fig. 3 shows the PE powder grains and their aggregates for three representative samples characterized by the lowest (1), moderate (3) and highest (8) transmittance limit.

Electron microscope images of all PE powders studied in this work are given in Supplementary data. When estimating particle size we take into account the dimensions of PE grains, but not their aggregates, because the aggregates can be compressed well during pellet formation to uniformly pressed grains and the grains themselves and the voids between them are expected to be relevant to the light scattering processes. However, in some cases
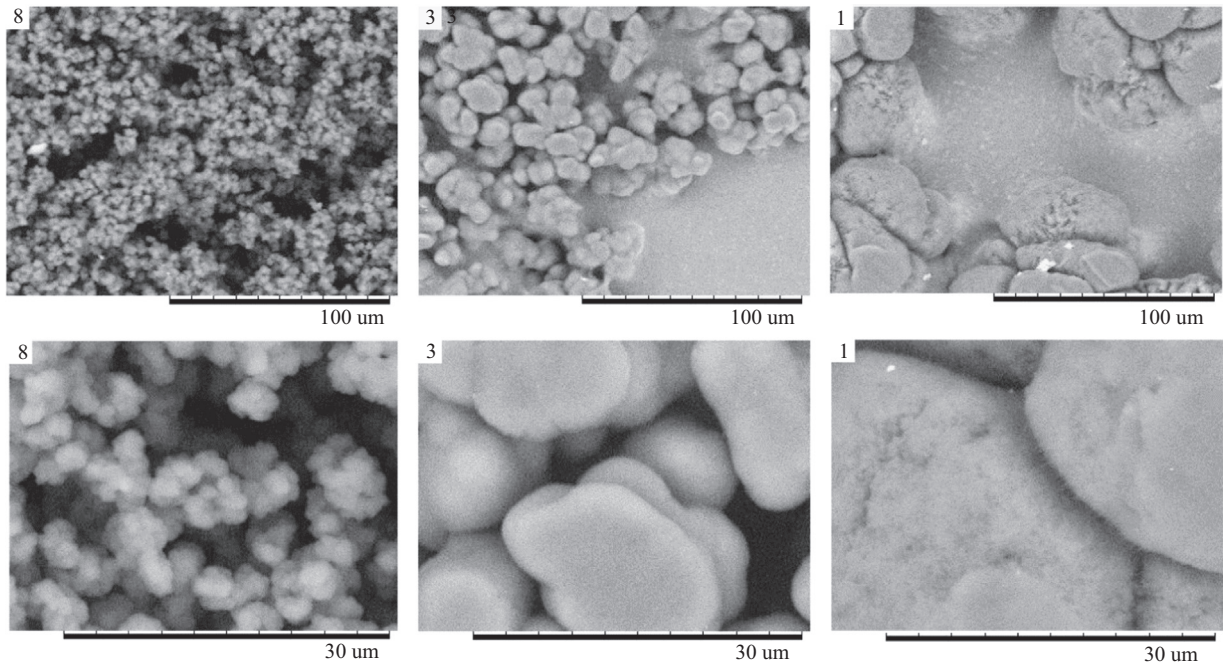
Fig. 3. Electron microscope images of PE sample nos. 1, 3, and 8 measured with magnification of 600 (top row) and 3000 (bottom row) times.

(e.g. sample 1) the distinction between grains and aggregates becomes ambiguous. The MPS-EM of the studied samples is listed in Table 1. One can see the inverse correlation of PE particle size with the PE transparency in the far-IR range, which is expected if light scattering by PE grains is considered as the main process limiting the resulting transmittance. Back to Fig. 2 and Table 1, taking into account this data one can choose an appropriate PE for pellet preparation, which allows measuring far-IR spectra with the required signal-to-noise ratio without necessity of pellet melting.

3.2. MPS-EM and MPS-SI comparison

As was shown in Section 2.4, the imaginary part of the effective refractive index of the PE pellet $\tilde{\kappa}(w)$ should have well-defined maximum, whose position in the spectra depends on the MPS of the corresponding PE powder. In order to obtain the imaginary part of the effective refractive index of the studied PE pellets (Fig. 4), their far-IR and mid-IR spectra joined together have been transformed according to Eq. (2).

The observed dependences support the scale-invariance rule, proposed in Section 2.4. In particular, apart from PE absorption bands the curve shapes are geometrically similar for all pellets. Therefore, light scattering by the PE grains is indeed the main reason limiting the overall transmittance of PE pellets in the far-IR range. Peak positions of the general trend were determined by manual inspection (results are given in Table 1); the uncertainty is relatively large when those peaks overlap with absorption lines. Using results for pellet 1 we obtain $A=1.1$, which is further used to estimate MPS-SI in all pellets (see Table 1). We show calculation uncertainties
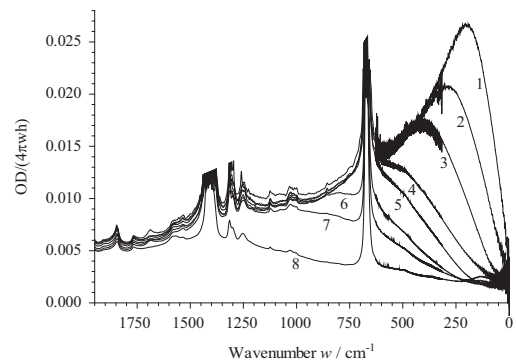
Fig. 4. Imaginary part of the effective refractive index $\tilde{\kappa}(w)$ calculated from combined far- and mid-IR spectra of PE pellets.

neither for A nor for obtained MPS-SI, because much greater uncertainties are inherent in both the "effective" definition of this MPS-SI and the scale-invariance approach itself.

There is a qualitative agreement between the MPS-EM and MPS-SI data; in particular, they show the same trend. However, the quantitative differences are up to four times for fine powders. We attribute this difference to the different sizes sensed by the two methods. Our processing algorithm of electron microscope images determines the MPS of compact grains, while the MPS-SI may correspond to larger aggregates if they are densely packed. Another ambiguity comes from the arbitrary choice of the reference sample for determination of constant A. We chose sample 1, since its individual grains are visually separated from each other to the largest extent (Fig. 3); however, the morphology of samples 1 and 2 is a bit different from

others samples (see images in Supplementary data). Overall, we conclude that the (dense) aggregation of grains has a more pronounced effect on the spectra of finer powders.

In principle, it is possible to associate the MPS-EM with aggregates instead of individual grains. In particular, this will lead to values of 90 and 8 μm for samples 1 and 8, respectively (Fig. 3), which in turn will improve the agreement with the MPS-SI (rescaled appropriately). However, we leave this analysis for a further study, because (1) the identification of aggregates is even more ambiguous than that of single grains; (2) images do not exactly correspond to the morphology (packing) of the pellet, which could be fixed by preparing thin sections of the pellet.

3.3. Criterion for PE powder to be suitable for far-IR spectroscopy

Polyethylene is a widely used plastic which is mainly classified by molecular chain length, material density and branching. Taking into account that the light wavelength in far-IR range is a few orders longer than the single PE molecule (even in the case of UHMWPE), the above-mentioned parameters seem to be irrelevant for selection of PE powder regarding its pellet transparency in far-IR range. As was shown above, the overall transparency of the PE pellet in far-IR range is inversely proportional to MPS of its PE powder, where MPS corresponds to the size of compact PE grains. In this sense the properties of the used catalyst and synthesis conditions play crucial roles in the far-IR transparency of PE, while, for example, the resulting molecular chain length is a secondary consequence of those conditions.

Finding optimum PE powder for particular experiment requires a trade-off between sufficient transparency in far-IR range (Table 1) and the availability/price of the corresponding PE. On the one hand, Table 1 shows that the finer the PE powder, the better it is for far-IR spectroscopy. On the other hand, the synthetic procedure used in this work becomes significantly more complicated for smaller MPS of PE powder produced, because (see Eq. (A1)): (1) synthesis of fine PE powder requires fine catalyst powder, and (2) the resulting PE yields are quite low. Indeed, while PE sample 1 was produced using catalyst of MPS ~4.5 μm with the yield of 12 kg per g of catalyst (typical for PE production), the PE sample 8 was produced using catalyst of MPS ~0.3 μm only (15 times smaller) with the yield of 0.7 kg per g of catalyst (almost 20 times less). Further decrease of these parameters seems to be either hardly feasible (MPS of catalyst) or unpractical (due to small dependence between PE yield and its MPS). Thereby, estimating the upper limit for MPS of PE powders from Table 1, one concludes that the PE pellet of typical thickness of ~0.5 mm is expected to be transparent enough in the far-IR range if the MPS of PE grains is ~4 μm or less. Of course, this is approximate estimation, since the overall PE pellet performance depends not only on the MPS of individual grains but also on the density and size of their aggregates. Taking this into account, the above mentioned upper limit of MPS of PE powders which are expected to be transparent enough in the far-IR can be extended to the range roughly defined as 2–10 μm. It

should be mentioned that the quantitative estimation of the far-IR spectra (or MPS-SI) from the electron microscope images does not seem feasible without tedious radiative transfer simulations based on realistic sample morphology.

4. Conclusions

Applying different catalysts and changing the time of polymerization reaction a set of PE powders of different PE particle size was synthesized. The transmission spectra of PE pellets made of these powders at room temperature were measured in far-IR range. It was shown that the overall transparency of the PE pellet in far-IR region is inversely proportional to the MPS of PE grains. The imaginary part of the effective refractive index of the studied PE pellets obeys light-scattering scale invariance rule, indicating that the transmission of PE pellets is limited by light scattering by PE grains. PE powders with MPS of ~4 μm or less are found to be suitable as a matrix for pellet formation in far-IR spectroscopy without the necessity of pellet melting.

Appendix A. relation between MPS of catalyst and PE particles

Assuming that the PE particle is formed around the particle of catalyst, the MPS of PE and catalyst are bound by the following equation [15,22]:

$$D^{50}(\text{PE}) = D^{50}(\text{ct}) \cdot \sqrt[3]{G\frac{\rho_{\text{ct}}}{\rho_{\text{PE}}} + 1}, \tag{A.1}$$

where $D^{50}(\text{PE})$ is the MPS of PE particles, $D^{50}(\text{ct})$ is the MPS of catalyst particles, G is a polymer yield (g PE per g catalyst) and ρ_{PE} and ρ_{ct} are the densities of PE and catalyst, respectively.

Appendix B. Supporting information

Supplementary data associated with this article can be found in the online version at http://dx.doi.org/10.1016/j.jqsrt.2014.05.011.

References

[1] Weinberger P, Grunert M. Variable temperature far and mid FT-IR as a valuable tool to determine the spin transition temperature of iron

(II) spin-crossover coordination compounds. Vib Spectrosc 2004;34: 175–86.

[2] Dumelow T, Parker TJ, Smith SRP, Tilley DR. Far-infrared spectroscopy of phonons and plasmons in semiconductor superlattices. Surf Sci Rep 1993;17:151–212.

[3] Fumino K, Wulf A, Ludwig R. The cation–anion interaction in ionic liquids probed by far-infrared spectroscopy. Angew Chem Int Ed Engl 2008;47:3830–4.

[4] Kendix E, Moscardi G, Mazzeo R, Baraldi P, Prati S, Joseph E, et al. Far infrared and Raman spectroscopy analysis of inorganic pigments. J Raman Spectrosc 2008;39:1104–12.

[5] Kendix EL, Prati S, Joseph E, Sciutto G, Mazzeo R. ATR and transmission analysis of pigments by means of far infrared spectroscopy. Anal Bioanal Chem 2009;394:1023–32.

[6] Barish WB, Behnke GT, Nakamoto K. Laboratory preparation of polyethylene pellets. Appl Spectrosc 1968;22:337–8.

[7] Ovcharenko VI, K. Yu Maryunina, Fokin SV, Tretyakov EV, Romanenko GV, Ikorskii VN. Spin transitions in non-classical systems. Russ Chem Bull Int Ed 2004;53:2406–27.

[8] Veber SL, Fedin MV, Maryunina KY, Boldyrev KN, Sheglov MA, Kubarev VV, et al. The influence of intense THz radiation on spin state of photoswitchable compound $Cu(hfac)_2L^{Pr}$. J Phys Chem A 2013;117:1483–91.

[9] Finch A. Chemical applications of far infrared spectroscopy. London: Academic Press; 277.

[10] Schiele C, KHalfar K. Cold pressing of polyethylene disk. A new technique. Appl Spectrosc 1965;19:163–4.

[11] Zakharov VA, Mikenas TB, Nikitin VE, Mozgunova NV. Catalyst and method of obtaining ultra-high molecular polyethylene using this catalyst. Russian Patent 2346006; 2009.

[12] Mikenas TB, Zakharov VA, Nikitin VE, Echevskaya LG, Matsko MA. New generation of supported Ziegler-type catalysts for polyethylene production. Russ J Appl Chem 2010;83:2210–9.

[13] Hock CW. How titanium chloride catalysts control the texture of as-polymerized polypropylene. J Polym Sci A – Polym Chem 1966;4: 3055–64.

[14] Boor Jr J. Ziegler–Natta catalysts and polymerizations. New York: Academic; 180.

[15] Bukatov GD, Zaikovskii VI, Zakharov VA, Kryukova GN, Fenelonov VB, Zagrafskaya RV. Morphology of polypropylene granulae and their relation with texture of titanium trichloride. Vysokomol Soedin Seriya A 1982;24:542–8.

[16] Forte MC, Coutinho FMB. Highly active magnesium chloride supported Ziegler–Natta catalysts with controlled morphology. Eur Polym J 1996;32:223–31.

[17] Mishchenko MI, Travis LD, Lacis AA. Scattering, absorption, and emission of light by small particles. Cambridge: Cambridge University Press; 2002.

[18] Birch JR. The far infrared optical constants of polyethylene. Infrared Phys 1990;30:195–7.

[19] Horwitz JW. Infrared refractive index of polyethylene and a polyethylene-based material. Opt Eng 2011;50:093603.

[20] Jaffer A. FreeSnell: polyethylene [Internet]. Available from: ⟨http://people.csail.mit.edu/jaffer/FreeSnell/polyethylene.html⟩ [cited 23.12.13].

[21] Bohren CF, Huffman DR. Absorption and scattering of light by small particles. New York: Wiley; 1983.

[22] Ruff M, Paulik C. Controlling polyolefin properties by in-reactor blending: 2. Particle design. Macromol React Eng 2013;7:71–83.